SECURITY INFORMATION

c. 2

[redacted]

Copy 44
RM SL53H11

RESEARCH MEMORANDUM

for the

Office of Chief of Ordnance, Department of the Army

FLIGHT INVESTIGATION OF NINE REDUCED-SCALE (1:3.75) HERMES A-2S ROCKET-MOTOR TEST VEHICLES

By Ralph A. Falanga

Langley Aeronautical Laboratory
Langley Field, Va.

NATIONAL ADVISORY COMMITTEE FOR AERONAUTICS

WASHINGTON

[redacted]

NATIONAL ADVISORY COMMITTEE FOR AERONAUTICS

RESEARCH MEMORANDUM

for the

Office of Chief of Ordnance, Department of the Army

FLIGHT INVESTIGATION OF NINE REDUCED-SCALE (1:3.75) HERMES A-2S ROCKET-MOTOR TEST VEHICLES

By Ralph A. Falanga

SUMMARY

Nine reduced-scale (1:3.75) Hermes A-2S rocket-motor test vehicles were flight tested at the Pilotless Aircraft Research Station, Wallops Island, Va. These tests were made to determine the motor performance characteristics under flight conditions at propellant preignition temperatures of -25° F, ambient temperature, and 130° F. All rocket motors functioned normally and performance was not adversely affected by accelerations encountered. Thrust, duration, and total impulse values obtained in flight were in reasonable agreement with those obtained in static tests.

For the models tested, the action time varied from 6.95 seconds to 9.95 seconds, the maximum acceleration from 15.3g to 21.1g, the maximum velocity from 3,040 feet per second to 3,440 feet per second, Mach number from 2.8 to 3.16, the average thrust from 1,960 pounds to 2,769 pounds, total impulse from 19,228 pound-seconds to 19,844 pound-seconds, the altitude attained from 32,300 feet to 40,800 feet, and the horizontal range from 30,300 feet to 42,600 feet.

INTRODUCTION

The Project Hermes is being conducted by the General Electric Company under the direction of the Office of Chief of Ordnance, Department of the Army. One phase of this program consists of the development of a short-range (75 nautical miles), surface-to-surface missile, which is to be propelled by a large single-stage, solid-fuel rocket motor. The solid-fuel propulsion system for this missile is being developed by the Thiokol Corporation, Redstone Division.

[redacted]

A number of successful static firings of ignition test motors and full-scale motors have been made (ref. 1). Successful static firings, however, are not always indicative of satisfactory flight performance because the propellant is not subjected to the acceleration loads which occur during launching and in flight. Excessive acceleration loads may cause propellant breakup or a shearing of the bond between the propellant and case wall, either of which may result in abnormal operation and subsequent motor destruction.

Since the extremely large size of the full-scale motors makes full-scale testing costly and difficult, a reduced-scale (approximately one-quarter) dynamic model of the full-scale motor was designed for flight testing. Thrust, acceleration, propellant configuration, and mass distribution were scaled by the Thiokol Corporation so that the propellant stresses encountered would be similar to those which would be encountered during launching and in flight of the full-scale motor.

Since propellant physical properties vary widely as a function of propellant temperature, flight tests must be made over the same range of propellant preignition temperatures to which the actual motors will be exposed during service.

At the request of the Office of Chief of Ordnance, Department of the Army, flight tests of nine reduced-scale models of the full-scale Hermes A-2S propulsion system were conducted at the Pilotless Aircraft Research Station, Wallops Island, Va. Three tests were conducted at each of propellant preignition temperatures of -25° F, ambient temperature, and 130° F. The results of these tests are given in the present report.

SYMBOLS

a	acceleration, ft/sec^2
g	acceleration due to gravity, 32.17 ft/sec^2
D	drag, lb
C_D	drag coefficient, D/qS
V	flight velocity, ft/sec
M	Mach number
t	time, sec
F	thrust, lb

W weight, lb

W_i instantaneous weight, lb

θ flight-path angle, deg

S cross-sectional area, sq ft (0.372 sq ft)

q dynamic pressure, $\frac{1}{2}\rho V^2$, lb/sq ft

ρ air density, slugs/cu ft

Description of Rocket Motor

Details of the rocket motor are shown in figure 1. A polysulfide-perchlorate rubber-base propellant of T-13/E2 composition was used in the reduced-scale models tested. The polysulfide-perchlorate propellants weighed approximately 95.5 pounds and were internal-burning charges. An axial perforation which incorporated the design of five rounded star points extended throughout the chamber to a point near the hemispherical head. This configuration allows nearly constant combustion pressures and a negligible displacement of the center of gravity of the propellant during the burning period (refs. 1 and 2). All outer surfaces of the charge were lined with an inhibitor which also bonded the propellant charge to the steel chamber.

The light-weight motor cases were fabricated from SAE 4130 steel and normalized to provide a minimum tensile yield strength of 75,000 psi. The case was 8.265 inches in diameter and had a cylindrical length of 31 inches and a wall thickness of 0.0625 inch for both the cylindrical and forward head portions. The weight was approximately 28.5 pounds.

The test nozzles were machined from SAE 1020 steel bar and had a throat section of solid carbon which was press fitted and machined in place. The nozzle had an expansion ratio of 7.8 and weighed approximately 7.5 pounds.

DESCRIPTION OF THE MODEL

The flight-model body consisted of the T-40H reduced-scale Hermes A-2S test motor described in the previous section. Affixed to the motor was a nose and tail section as illustrated in figure 2. The nose and tail assemblies were designed to meet the minimum structural and aerodynamic requirements of the test vehicles, because the sole purpose of this investigation was to evaluate the propellant and its design under flight conditions. The nose assembly was a rolled aluminum cone-cylinder combination with bulkheads to provide stiffness. Sufficient lead ballast was added to the nose to give the model the necessary aerodynamic stability. The tail assembly was a rolled aluminum cylinder with stiffening rings to which channels were attached for the purpose of securing the four equally spaced stabilizing fins. The fins were 3/8-inch aluminum plate with a beveled leading edge. The plan form was a 30° delta with 0.549 square foot of exposed area per fin.

Average take-off weight for the models was approximately 167.5 pounds, while the average weight at burnout was approximately 72.0 pounds.

TEST CONDITIONS

In order to evaluate motor performance over a wide range of operating conditions, three models were temperature conditioned at -25° F (cold models), three at 70° F (ambient models), and three at 130° F (hot models). Temperature saturation of the propellant was accomplished by storing the cold models in a refrigerator and the hot models in a heater box for at least 20 hours prior to firing.

TEST TECHNIQUES

The models were launched from a near-zero-length launcher at a 70° elevation angle. Figure 3 shows the launcher and model prior to firing. The launcher consists of a T-shaped base with a pivoted boom and an adjusting beam. A disappearing lug which was installed in the nose assembly supported the model at the front end. Two clevis bolts with aluminum rivets supported the model at the back end. The aluminum rivets were designed to shear at approximately 1,000 pounds of thrust, in order to insure that the model was not prematurely launched because of possible erratic ignition.

A 100-watt CW Doppler radar unit tracked the models to obtain a velocity time history of the flight. An SCR 584 radar unit tracked the models to obtain altitude, horizontal range, and azimuth data. Standard radiosondes were released immediately before or immediately after each group of flights to obtain prevailing atmospheric conditions. A description of the CW Doppler radar unit and its operations may be found in reference 3.

In order to obtain details of the motion of the test vehicles leaving the launcher to insure that the stabilizing fins cleared the components of the launcher, two cameras were located in the immediate vicinity of the launcher. Tracking cameras also recorded the launching and flight paths of all the models. Motion pictures provided information pertaining to the stability of the flight models and revealed any irregularities which may have occurred during the thrusting period.

RESULTS AND DISCUSSION

A summary of the results of the test data obtained from the flight test vehicles is given in table I. Table II shows typical values which can be expected for the full-scale flight test motors at different temperatures.

Trajectories of the nine reduced-scale test vehicles obtained from the SCR 584 space radar unit are presented in figures 4, 5, and 6. Ground winds at the launching site were variable in direction with gusts up to 20 miles per hour. Differences in model trajectories are due mainly to these variable winds and to the crude construction of the models. The highest altitude reached was 40,800 feet obtained by one of the cold models, and the maximum horizontal range was 42,600 feet obtained by an ambient model. Because the SCR 584 radar unit lost track of two cold models and one hot model after they had reached their summit, complete information was not available for plotting their entire trajectories.

Figures 7, 8, and 9 show time histories of velocity and Mach number of the models as obtained from the Doppler radar data. Zero time on the graphs represents the time when iginition began. The hot models reached a maximum velocity of 3,420 feet per second, corresponding to a Mach number of 3.16. A minimum velocity of 3,040 feet per second, corresponding to a Mach number of 2.8, was reached by the cold models.

Acceleration time histories for the models were obtained by differentiating the velocity with respect to time and are presented in figures 10, 11, and 12. Maximum accelerations reached were 21.1g for the hot models, 20.45g for the ambient models, and 15.3g for the cold models. Data from zero time to approximately 2 seconds were not available for the acceleration curves because of the inability of the Doppler radar unit to track at close range.

The temperature-conditioned rocket motors functioned normally when subjected to the maximum acceleration loads encountered in flight with no adverse effects on performance.

The following longitudinal equation of motion was employed to obtain the drag on the models during coasting period:

$$D = -W\left(\frac{a}{g} + \sin\,\theta\right)$$

The assumption was made that the weight of the model at burnout and during the coasting period of the flight was equal to the inert materials of the model.

Figure 13 presents plots of the air density ρ and speed of sound V_c as a function of altitude, which were obtained from the radiosonde data at the time when the particular models were launched.

With the data obtained from the radiosonde record and from the SCR 584 radar unit, the drag on the models was converted into drag coefficient based on the projected frontal area (0.372 sq ft) of the models. This coefficient C_D is shown plotted as a function of flight Mach number in figures 14, 15, and 16.

Because there was still appreciable thrusting from the rocket motors after peak Mach numbers had been reached, it was not possible to calculate accurately the drag coefficient for this "tail-off" region (that duration from rocket-thrust termination to approximately 10 percent of the maximum thrust value). Hence the drag-coefficient curves were extrapolated as shown throughout the tail-off region of the rocket motors to give a more meaningful trend to the curves.

By using the following equation of motion, with successive approximation:

$$F = W_i\left(\frac{a}{g} + \sin\,\theta\right) + D$$

The thrust curves presented in figures 17, 18, and 19 were obtained. In the first approximation it was assumed that the propellant was expended at a constant rate, which was then modified by assuming a change of propellant weight proportional to total impulse. A second approximation was computed which closely approached the limits of the true conditions. Another assumption made in computing thrust was that at any Mach number the model drag coefficient during the thrusting period was equal to the drag coefficient during the coasting period. A calculation was made on model 1 using unpublished experimental base-pressure data on the differences between the power-on and power-off base drag. The differences in the two were indicated as being very small. It was felt that this check was sufficient to neglect any corrections to the total drag of the models since no provisions were made to measure base pressures.

The resulting thrust curves show that the variation for maximum thrust was from 3,160 pounds to 3,360 pounds for the ambient models (models 1, 2, and 3) from 3,290 pounds to 3,415 pounds for the hot models (models 4, 5, and 6) and from 2,688 pounds to 2,855 pounds for the cold models (models 7, 8, and 9). The extrapolated portions of the thrust curves from zero time to approximately 1 second were obtained from static firing data. The pronounced deviation which occurred between cold model 8 and the other two cold models was due to a difference in propellant temperature that existed prior to ignition. Model 8 was delayed for a longer time than normal on the launching site before firing, and this delay caused an increase in preignition propellant temperature which resulted in a higher maximum thrust and shorter action time than either of the other two cold models.

A comparison of thrust curves obtained from these flight tests with those from the Thiokol static test data conducted approximately at sea-level conditions is shown in figure 20. Static test data for an ambient motor were not available for comparison. In general, the results obtained from flight testing are in reasonable agreement with those from static testing.

Maximum variation of total impulse (measured in pound-seconds) based on action time was 3 percent for all the rocket motors flight tested, action time being that interval of the time when the thrust was greater than 10 percent of its maximum value. (See fig. 17.)

CAMERA STUDIES OF THE LAUNCHINGS

Figure 21 shows sequence photographs of the launching and initial portion of the flight path for an ambient model. Examination of the photographs did not reveal any signs of propellant failure for the model shown as well as for the other models tested.

CONCLUSIONS

Flight testing of the nine reduced-scale acceleration test vehicles indicated the following results:

1. At a preignition propellant temperature of 130° F, the rocket motors functioned normally under maximum acceleration loads of 21.1g.

2. Varying the preignition temperature from -25° F to 130° F caused no malfunctioning of the rocket motors.

3. Maximum thrust of 3,415 pounds occurred with a preignition propellant temperature of 130° F.

4. The thrust characteristics obtained from flight data were in reasonable agreement with the static results obtained by the manufacturer.

5. The maximum variation of total impulse was 3 percent for all the rocket motors flight tested.

Langley Aeronautical Laboratory,
National Advisory Committee for Aeronautics,
Langley Field, Va., August 11, 1953.

Ralph A. Falanga
Aeronautical Research Scientist

Approved: Joseph A. Shortal
Chief of Pilotless Aircraft Research Division

mhg

REFERENCES

1. Thackwell, H. L., Jr.: Development of 31-Inch Diameter Solid Propellant Rocket Motor for Hermes A-2 Missile. Rep. No. 28-51 (Contract No. DA-01-021-ORD-76, ORD Project TU1-2000C), Thiokol Corp., Redstone Div. (Huntsville, Ala.), Dec. 1951.

2. Williams, A. E.: Development of a 31-Inch Diameter Solid-Propellant Motor for the Hermes A-2 Missile. Rep. No. 5-53 (Contract No. DA-01-021-ORD-76, ORD Project No. TU1-2000C), Thiokol Corp., Redstone Div. (Huntsville, Ala.), Feb. 1953.

3. Welsh, Clement J.: Results of Flight Tests To Determine the Zero-Lift Drag Characteristics of a 60° Delta Wing With NACA 65-006 Airfoil Section and Various Double-Wedge Sections at Mach Numbers, From 0.7 to 1.6. NACA RM L50F01, 1950.

[redacted]

TABLE I

SUMMARY OF FLIGHT TEST RESULTS

	Ambient-temperature models (70° F)			Hot-temperature models (130° F)			Cold-temperature models (-25° F)		
	Model 1	Model 2	Model 3	Model 4	Model 5	Model 6	Model 7	Model 8	Model 9
Maximum altitude, ft	32,300	35,000	37,800	37,500	36,200	40,500	35,600	36,900	40,800
Horizontal range, ft	42,600	39,650	33,400	33,600	30,300	(Lost)	31,200	(Lost)	(Lost)
Acceleration at 1.8 sec, g units	16.0	16.9	18.2	18.2	18.2	18.6	11.2 (at 2.0 sec)	12.4 (at 2.0 sec)	11.5 (at 2.0 sec)
Maximum acceleration, g	18.3	20.1	20.45	20.45	20.45	21.1	15.4	15.3	15.3
Maximum velocity, ft/sec	3,230	3,320	3,380	3,420	3,420	3,440	3,030	3,060	3,040
Maximum Mach number	3.00	3.11	3.08	3.16	3.16	3.16	2.8	2.83	2.8
Maximum thrust, lb	3,160	3,310	3,360	3,290	3,415	3,415	2,750	2,835	2,688
Average thrust, lb	2,513	2,642	2,629	2,769	2,763	2,757	1,960	2,111	1,966
Action time[a], sec	7.65	7.45	7.38	6.95	7.0	7.0	9.9	9.4	9.95
Total impulse, lb-sec	19,228	19,684	19,404	19,246	19,344	19,304	19,404	19,844	19,568

[a]The interval of time when the thrust was greater than 10 percent of its maximum value. (See fig. 17.)

[redacted]

TABLE II

SUMMARY OF EXPECTED TYPICAL VALUES FOR

FULL-SCALE MOTORS

Operating temperature, °F	Action time, sec	Average thrust, lb	Total impulse, lb-sec
130	26.19	38,856	1,033,907
70	28.10	36,489	1,025,117
-25	36.57	28,633	1,017,700

NACA-Langley - 9-16-53 - 50

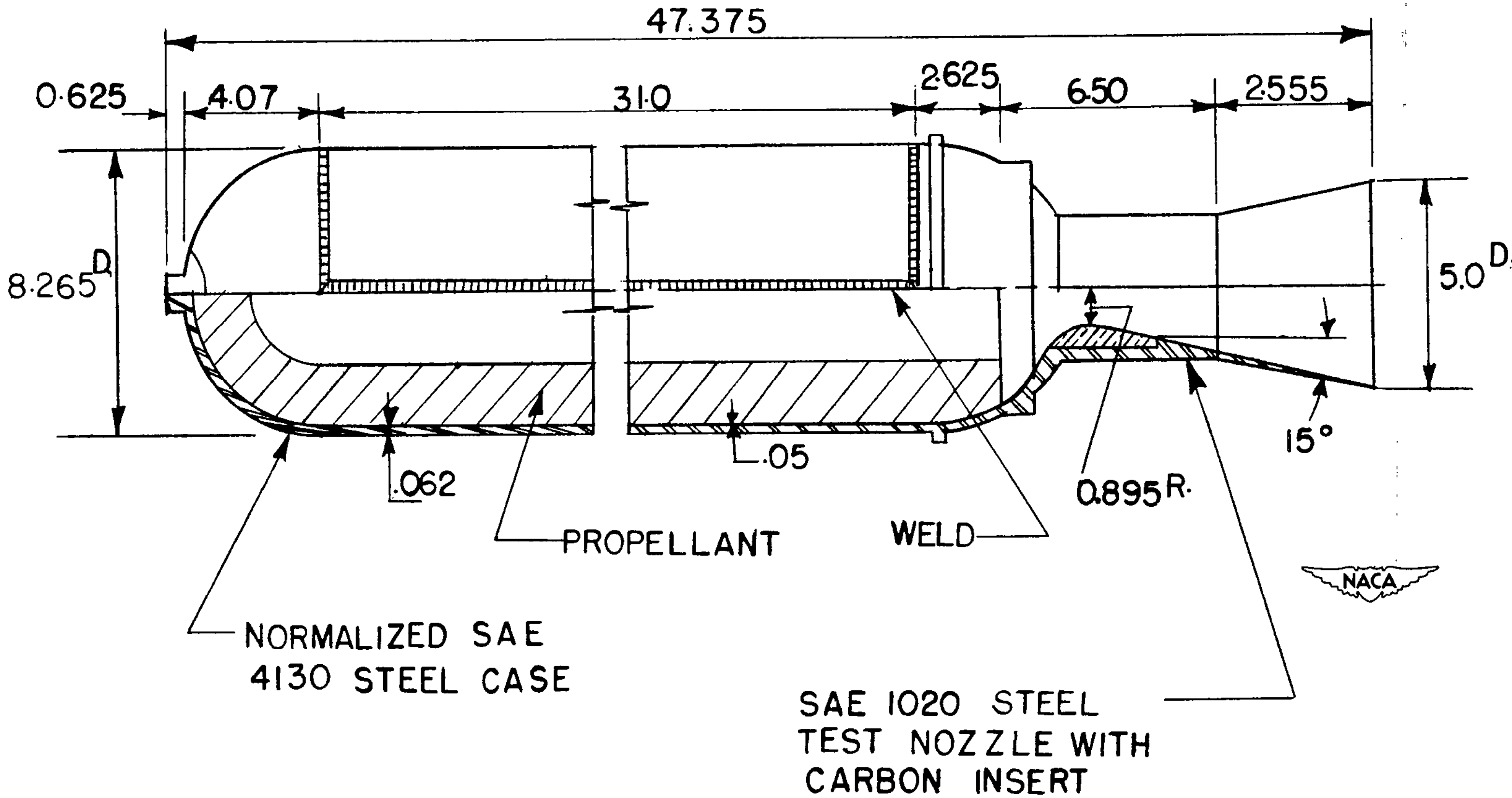

(a) Model configuration.

Figure 1.- Details of reduced-scale rocket motors. All dimensions are in inches.

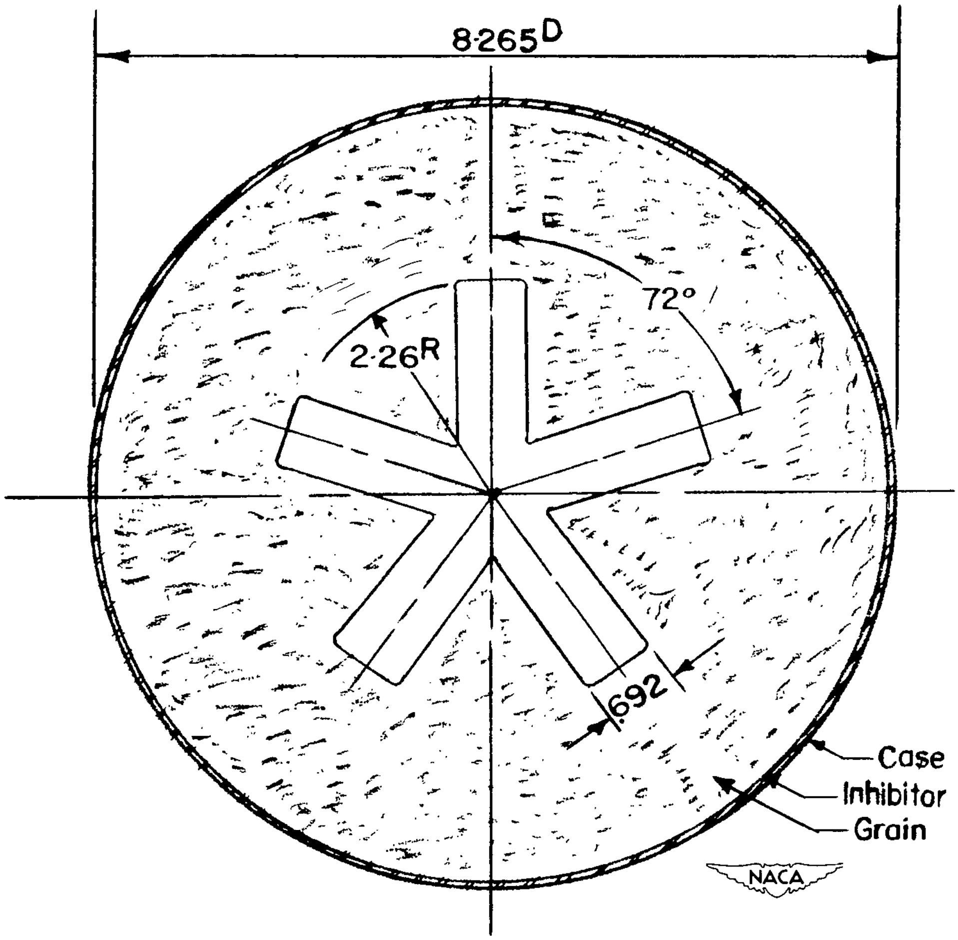

(b) Cross section of solid propellant for rocket motor.

Figure 1.- Concluded.

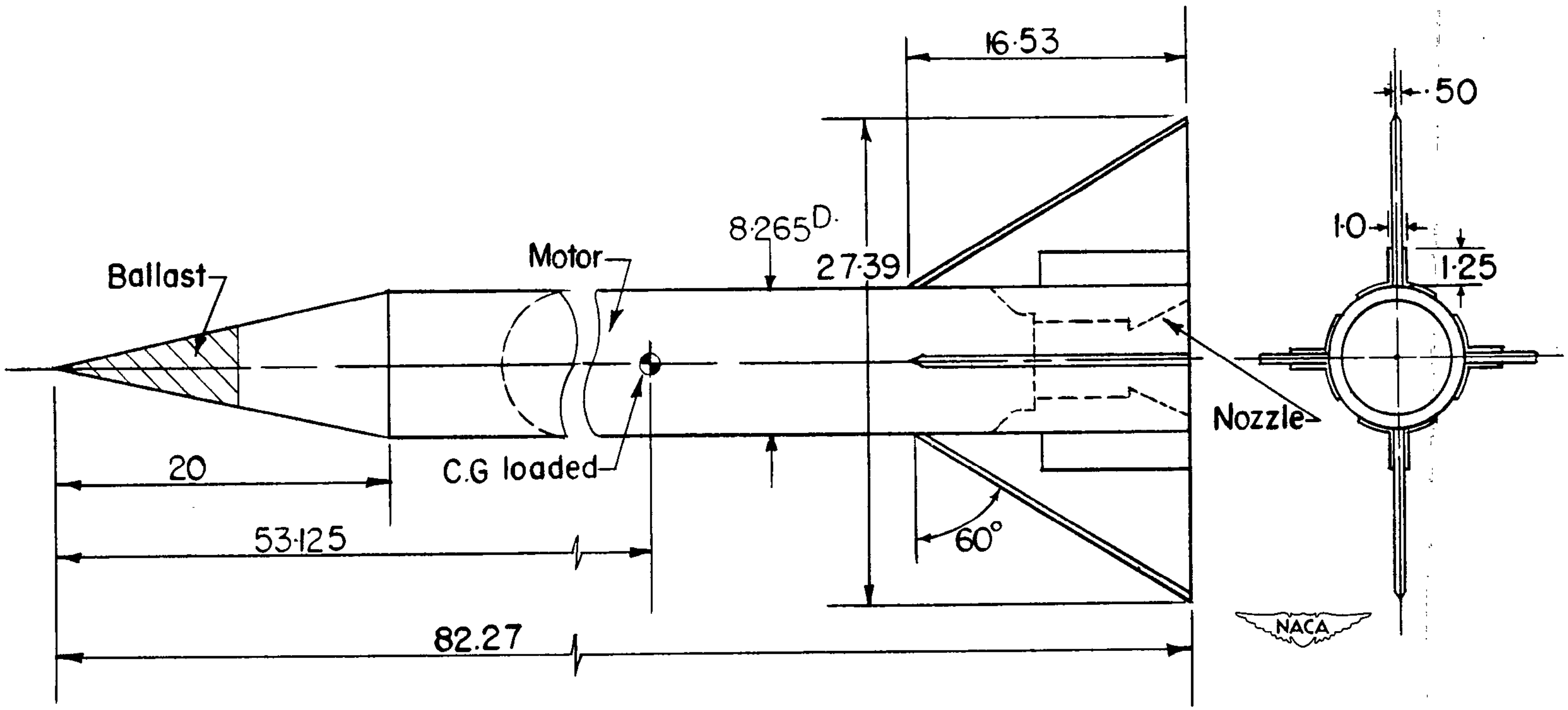

Figure 2.- External configuration of the flight test vehicle. All dimensions are in inches.

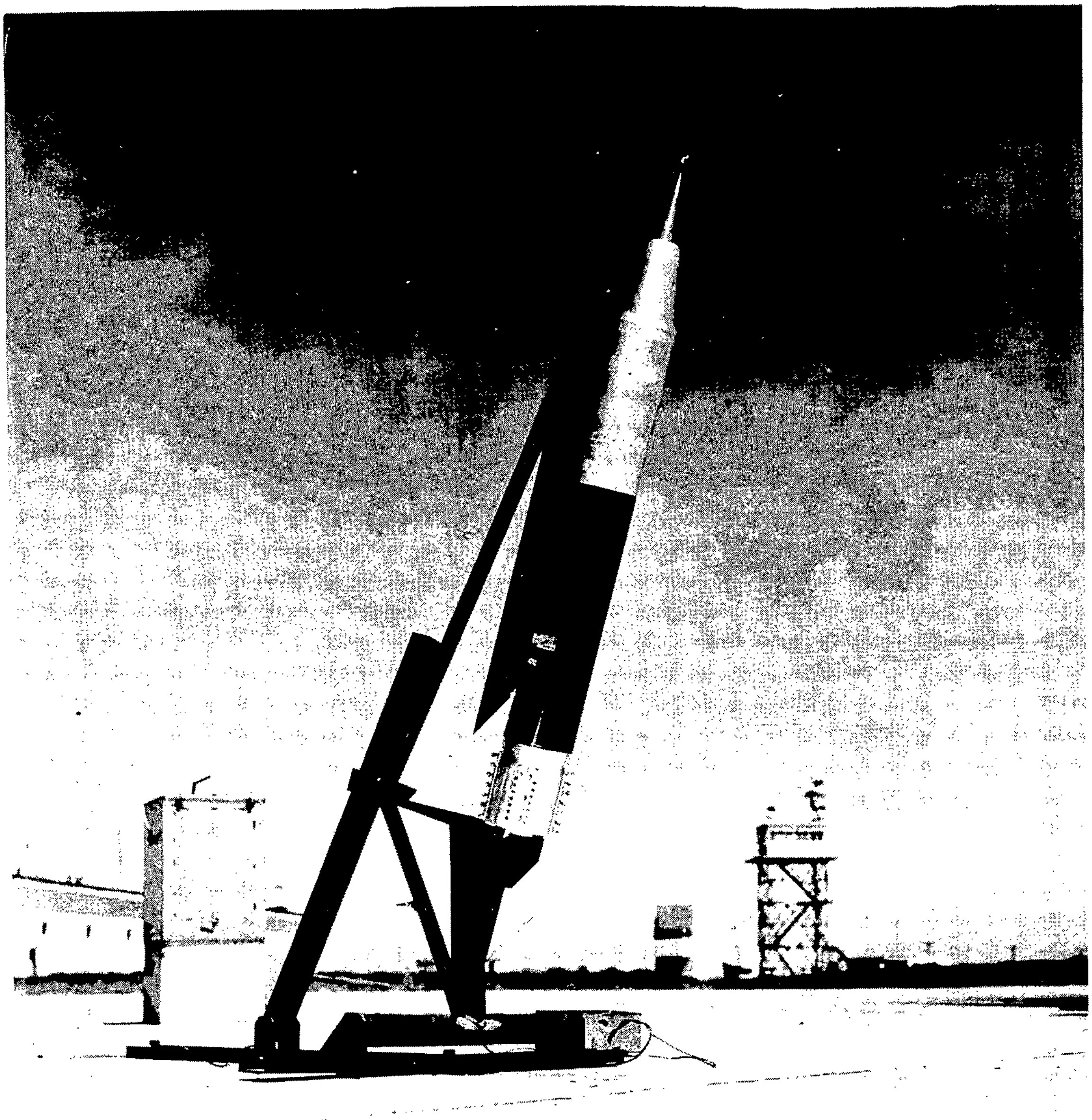

L-75549

Figure 3.- Flight model on launcher.

[redacted]

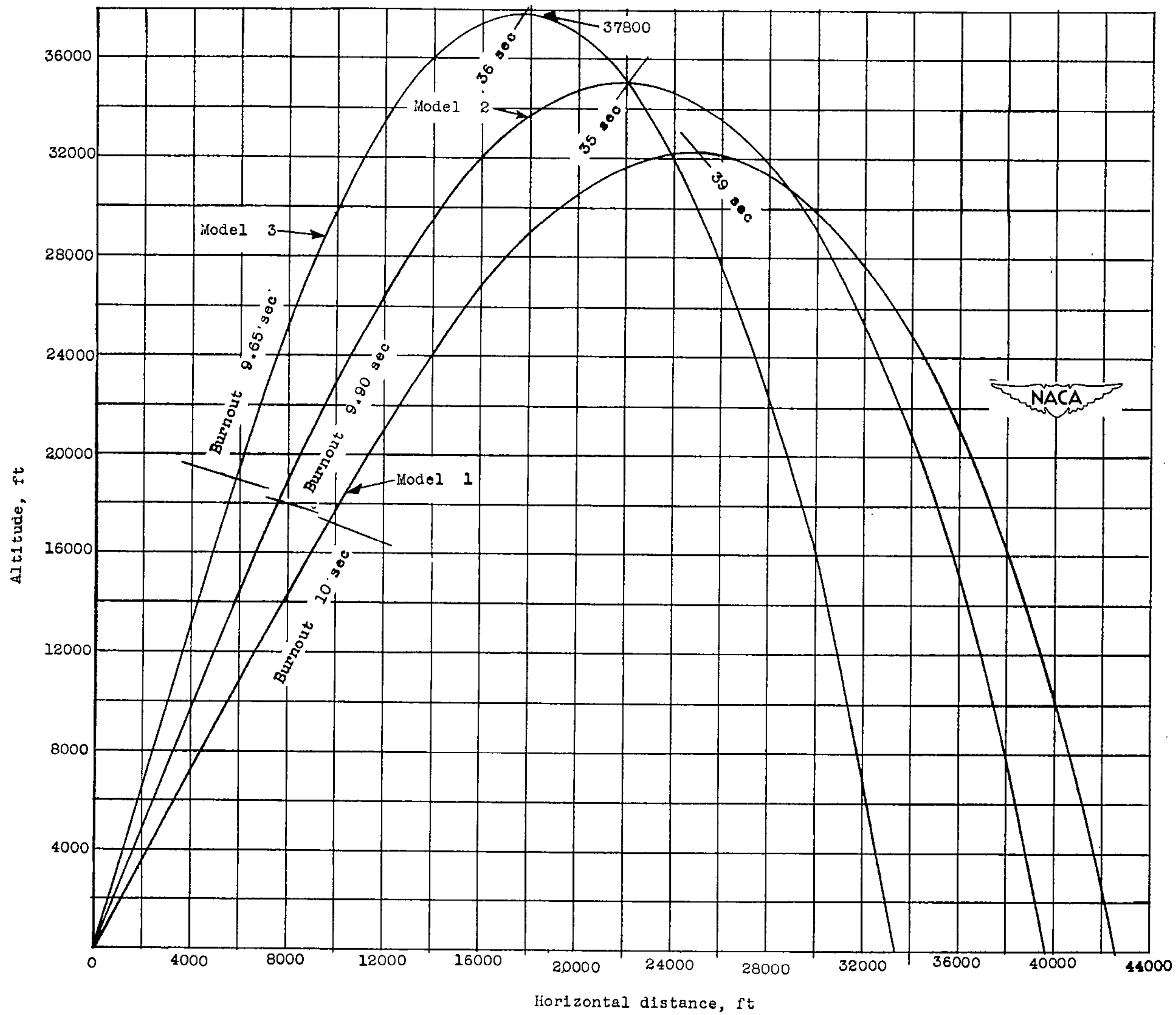

Figure 4.- Trajectories for ambient models (70° F).

[redacted]

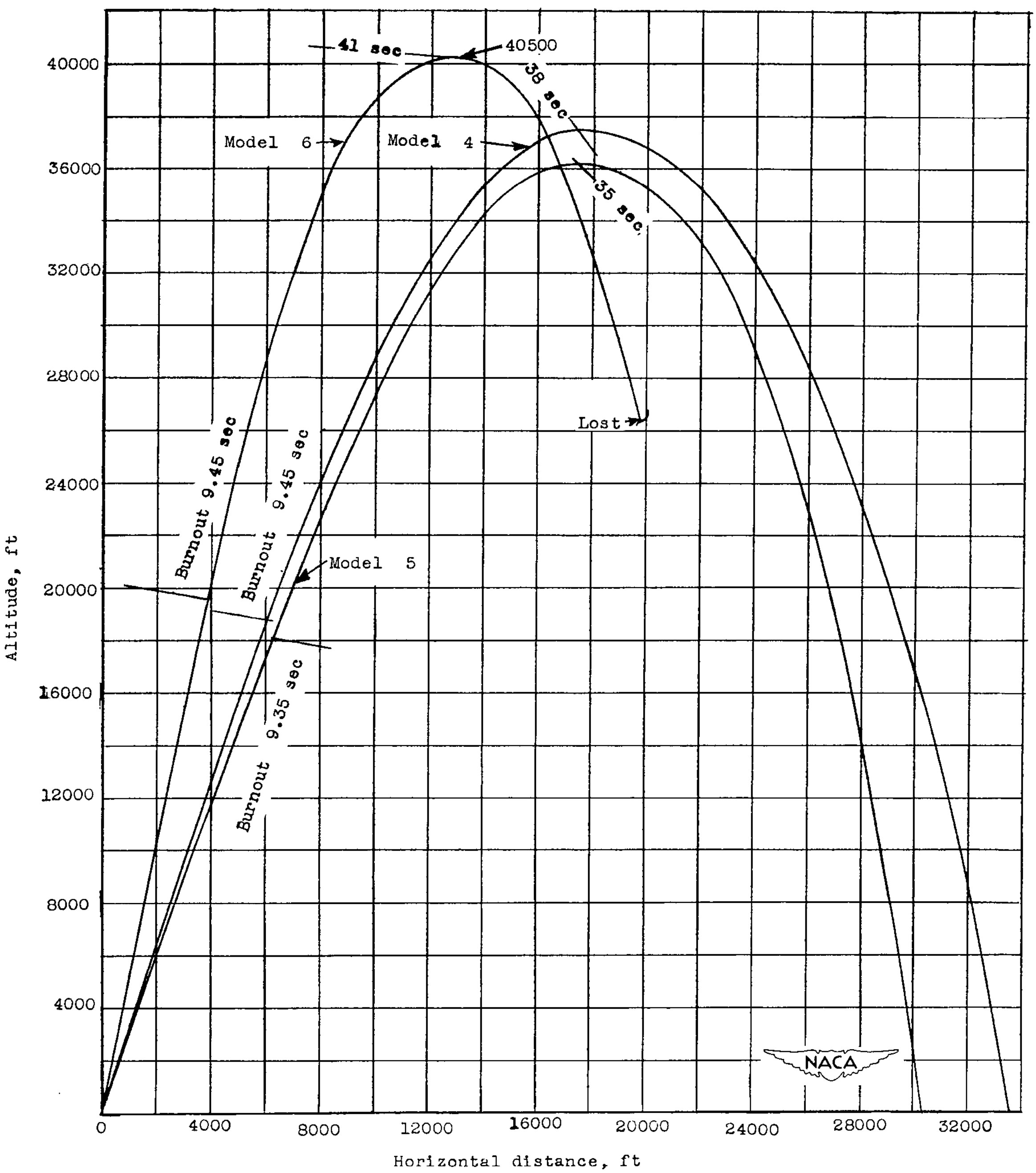

Figure 5.- Trajectories for hot models (130° F).

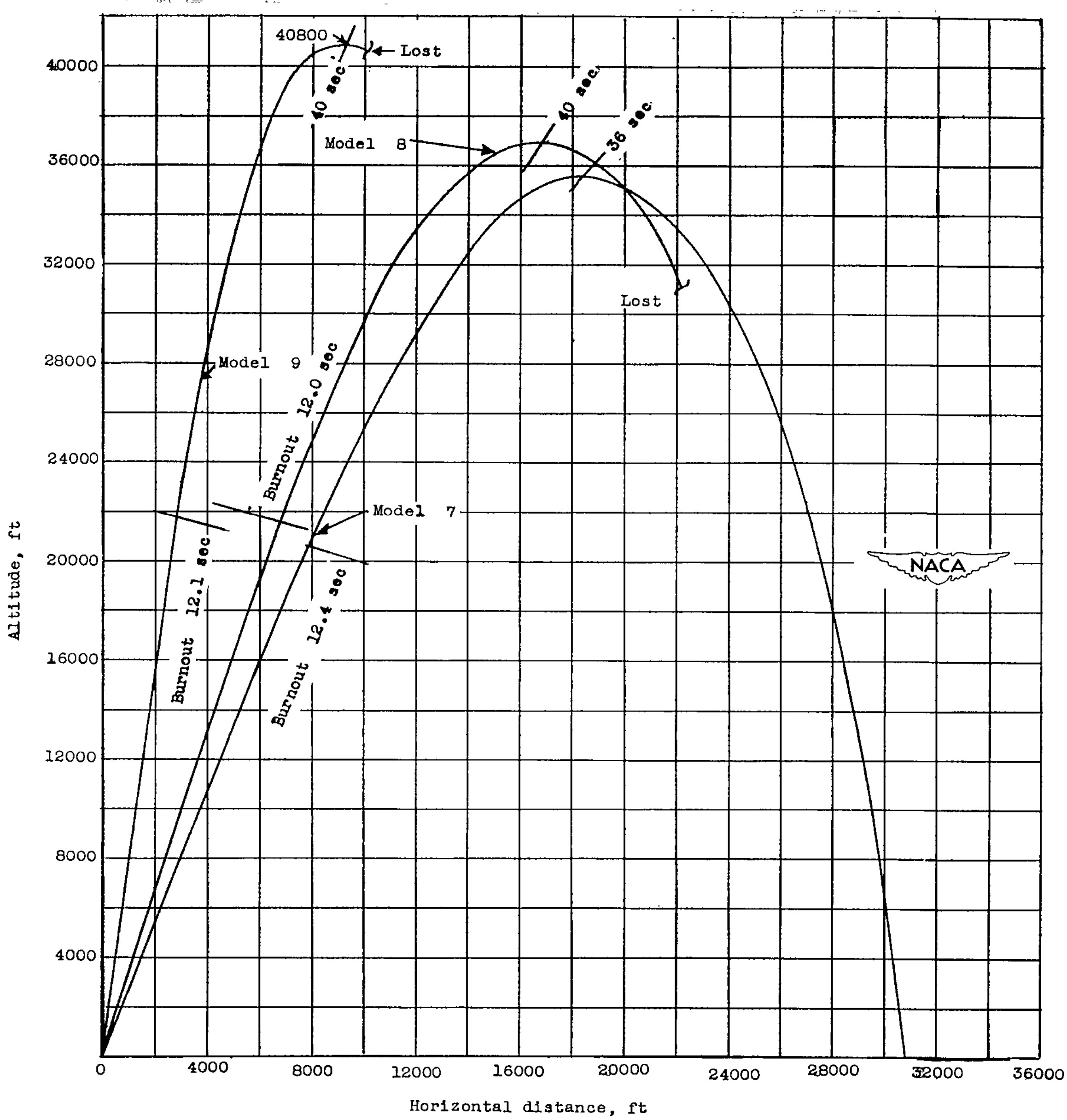

Figure 6.- Trajectories for cold models (-25° F).

[redacted]

[redacted]

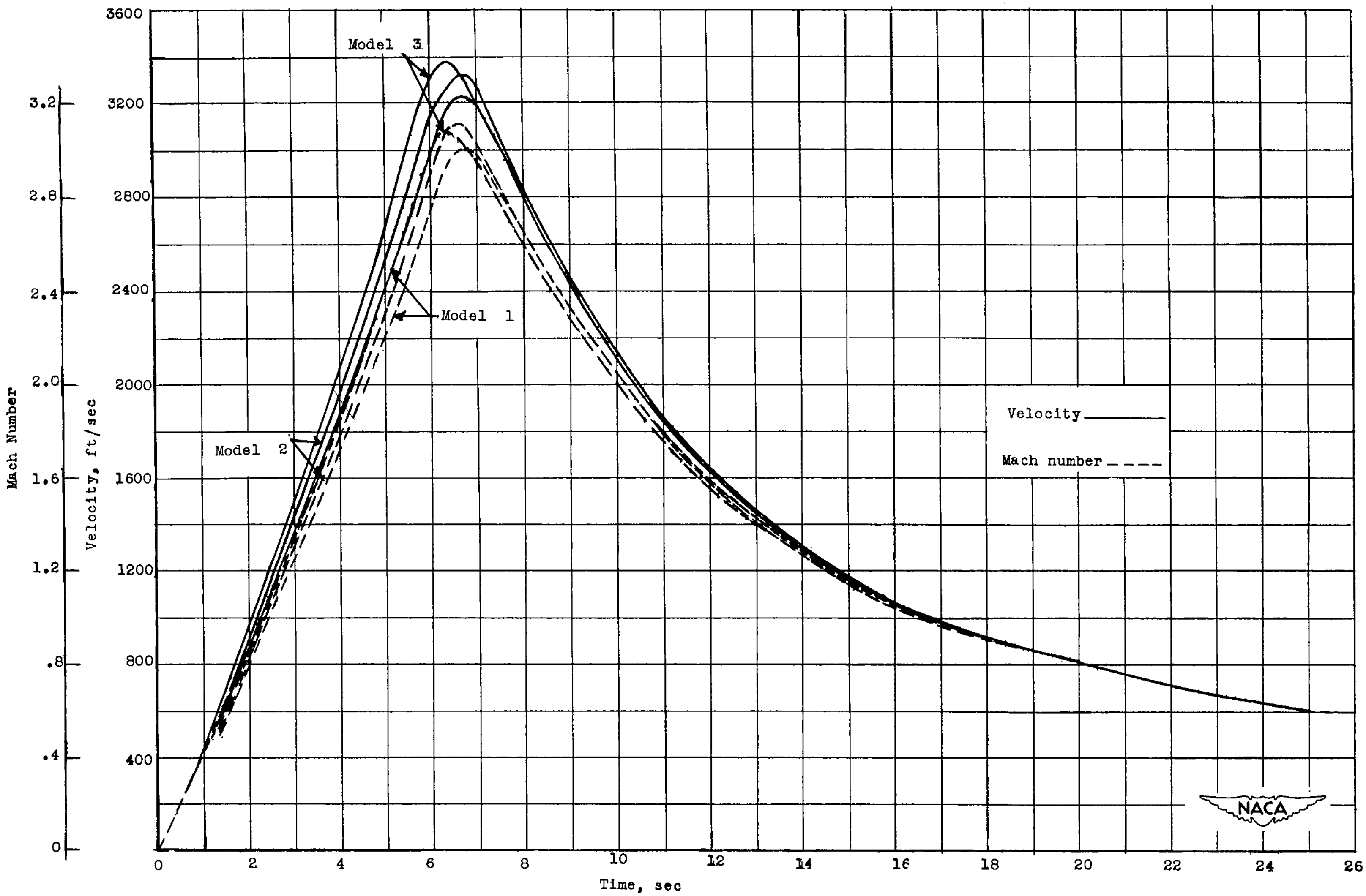

Figure 7.- Velocity and Mach number for ambient models as a function of time.

[redacted]

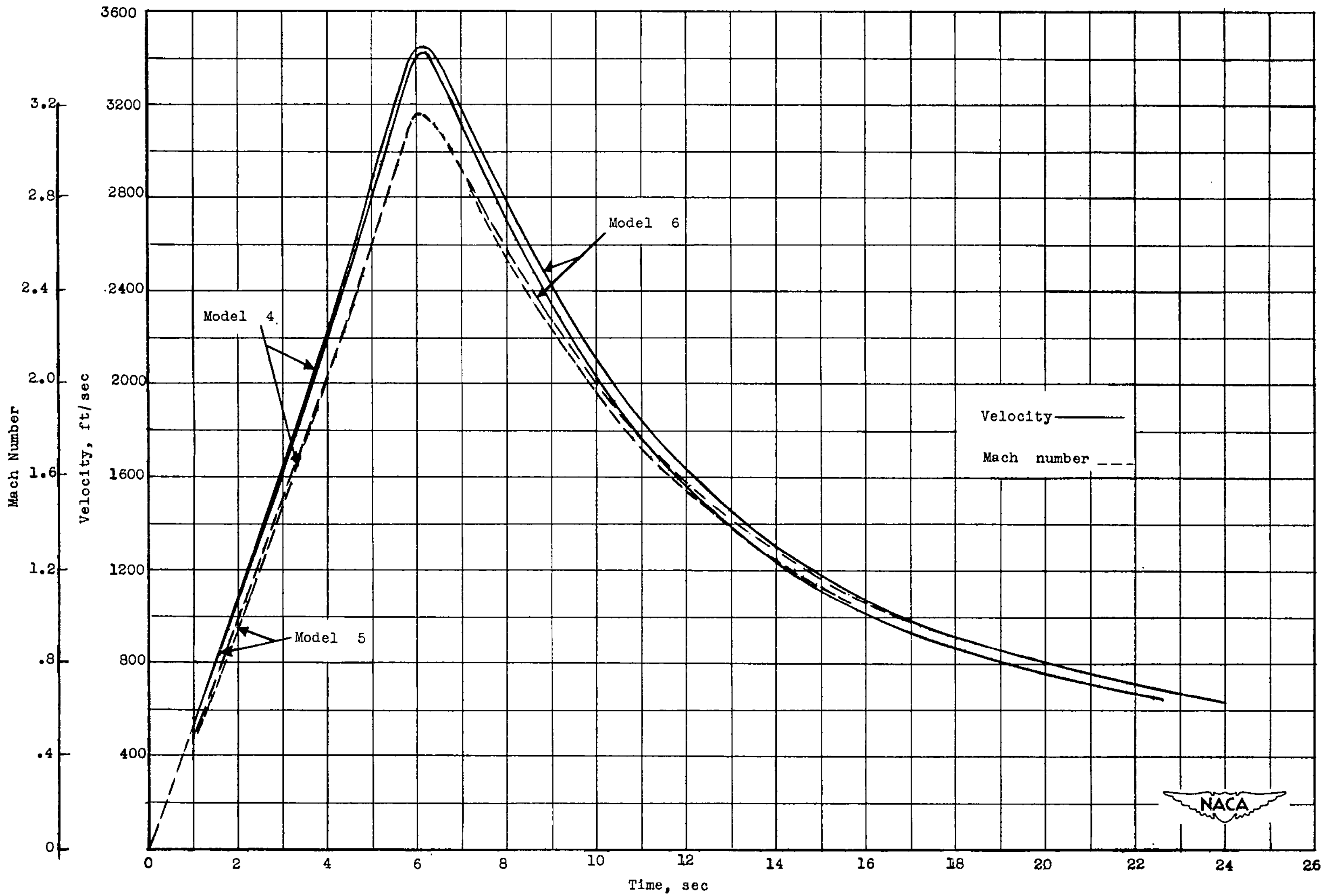

Figure 8.- Velocity and Mach number for hot models as a function of time.

[redacted]

[redacted]

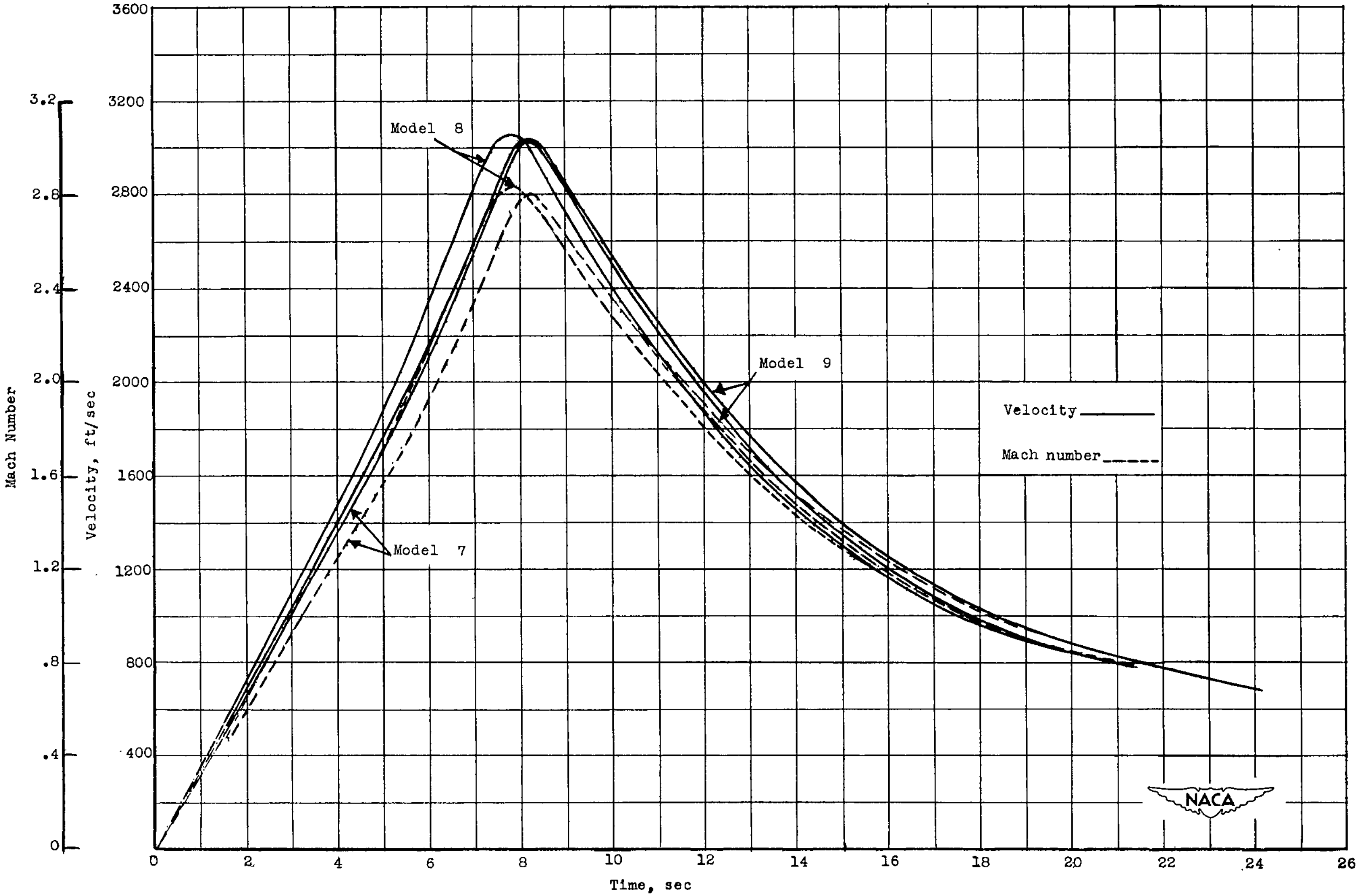

Figure 9.- Velocity and Mach number for cold models as a function of time.

[redacted]

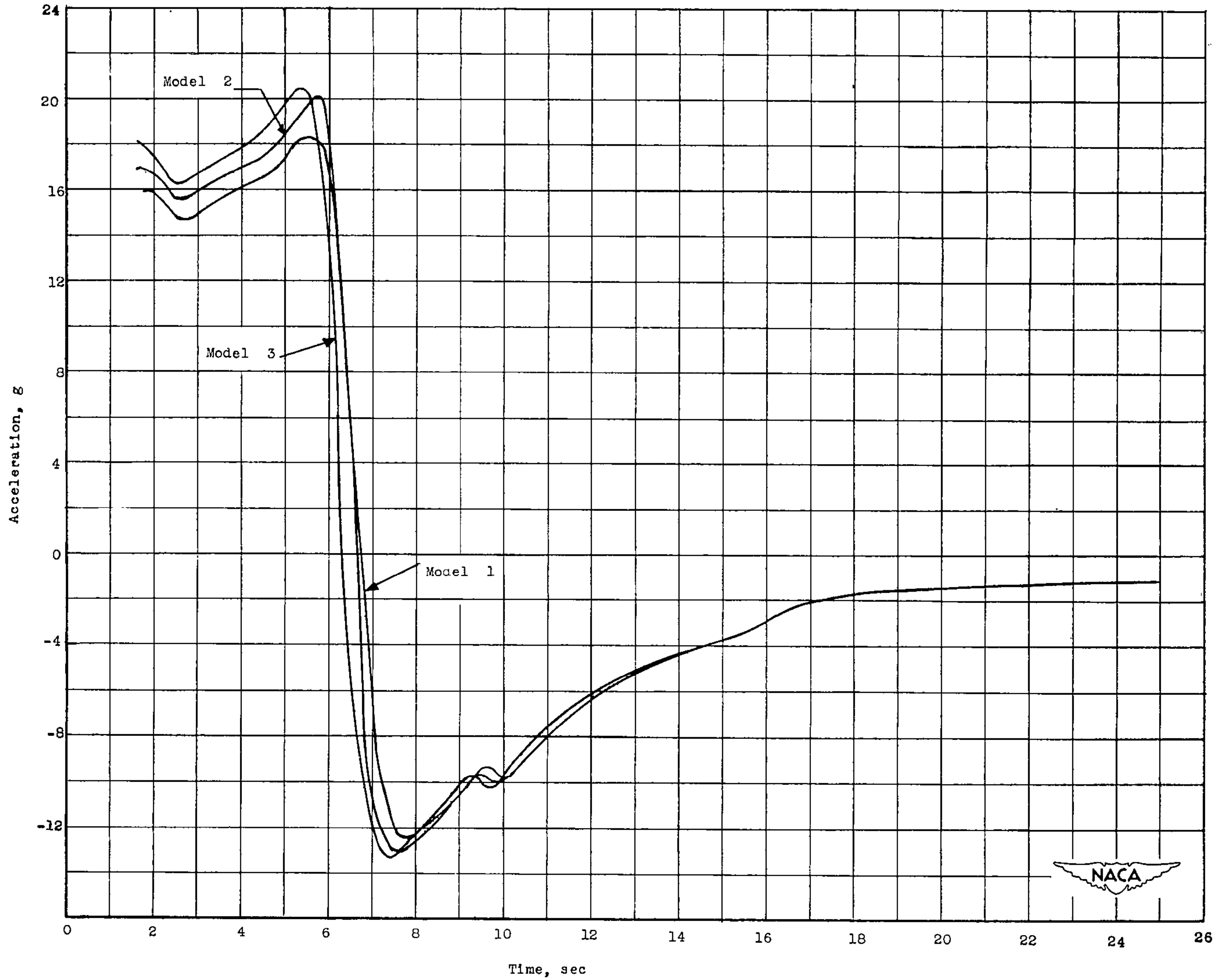

Figure 10.- Acceleration for ambient models as a function of time.

[redacted]

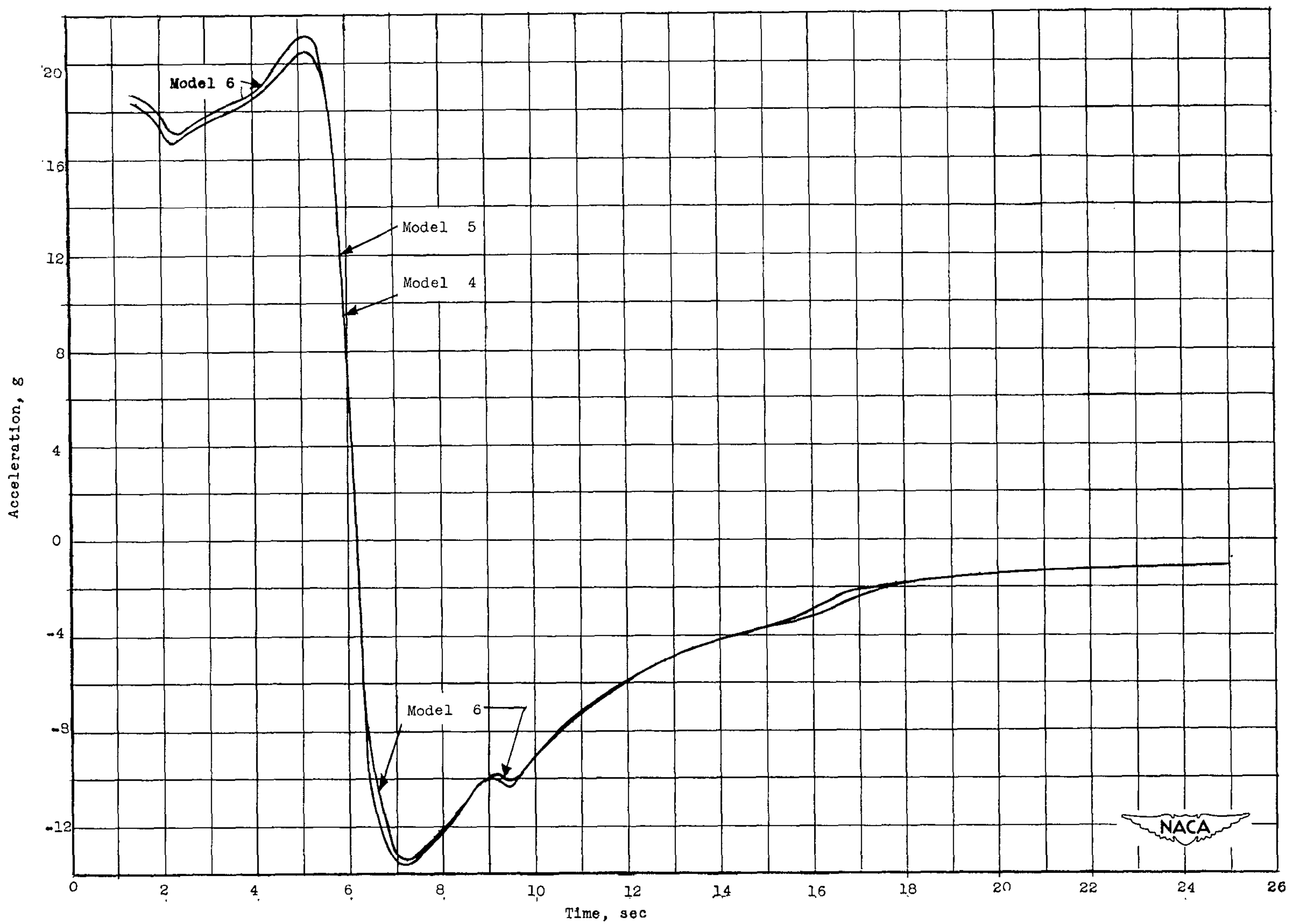

Figure 11. Acceleration for hot models as a function of time.

[redacted]

[redacted]

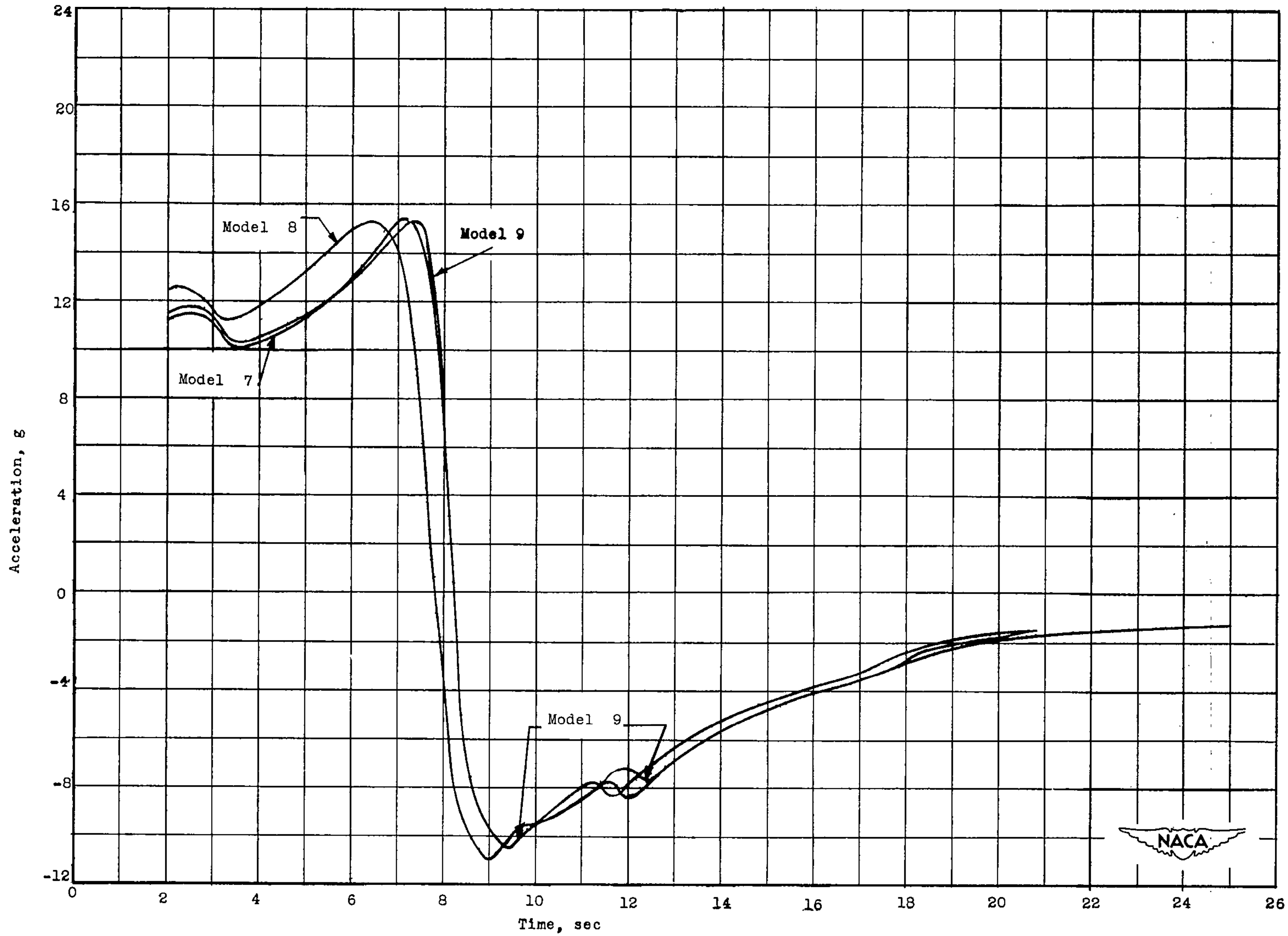

Figure 12.- Acceleration for cold models as a function of time.

[redacted]

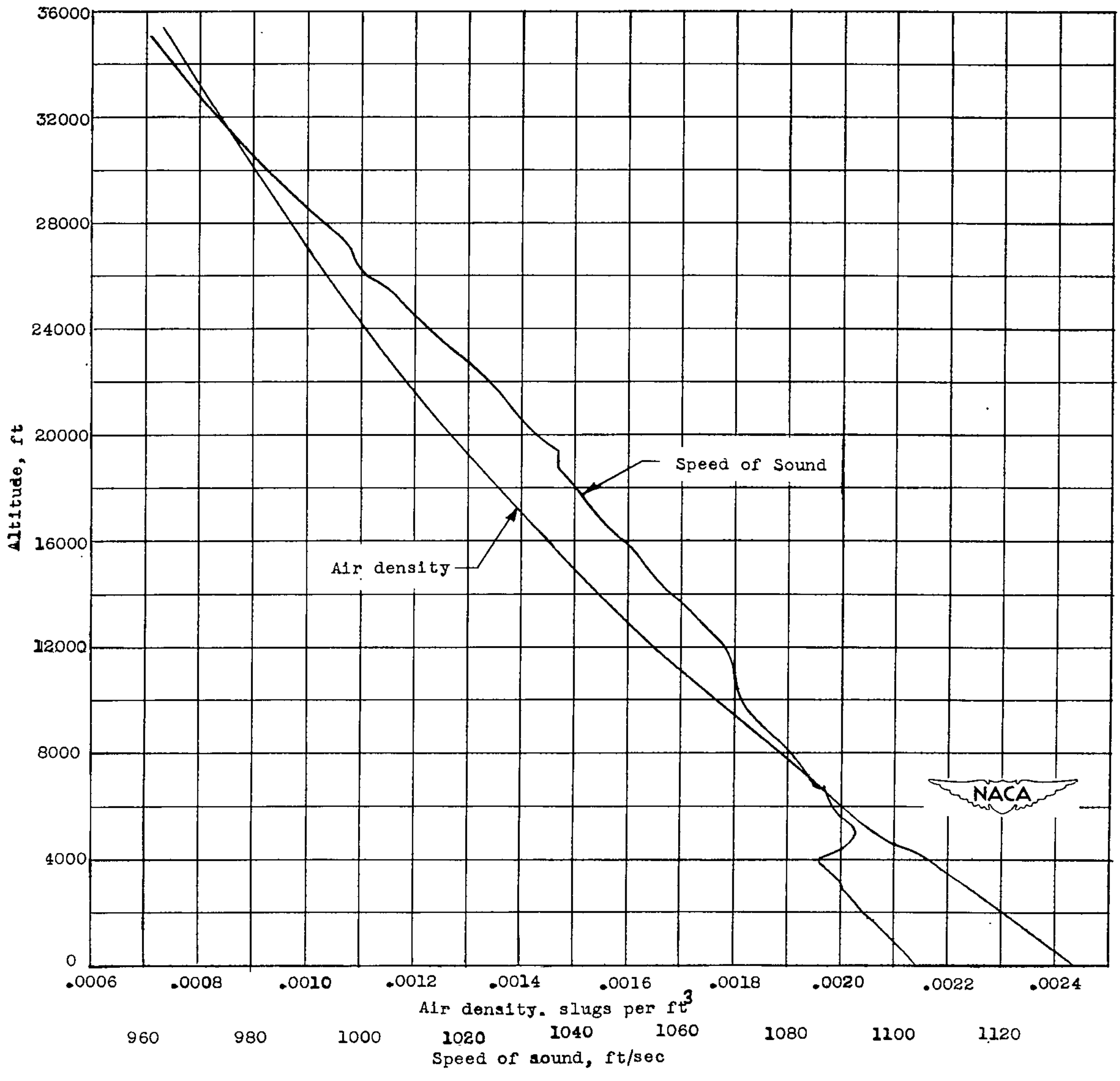

(a) Model 1.

Figure 13.- Air density and speed of sound as a function of altitude.

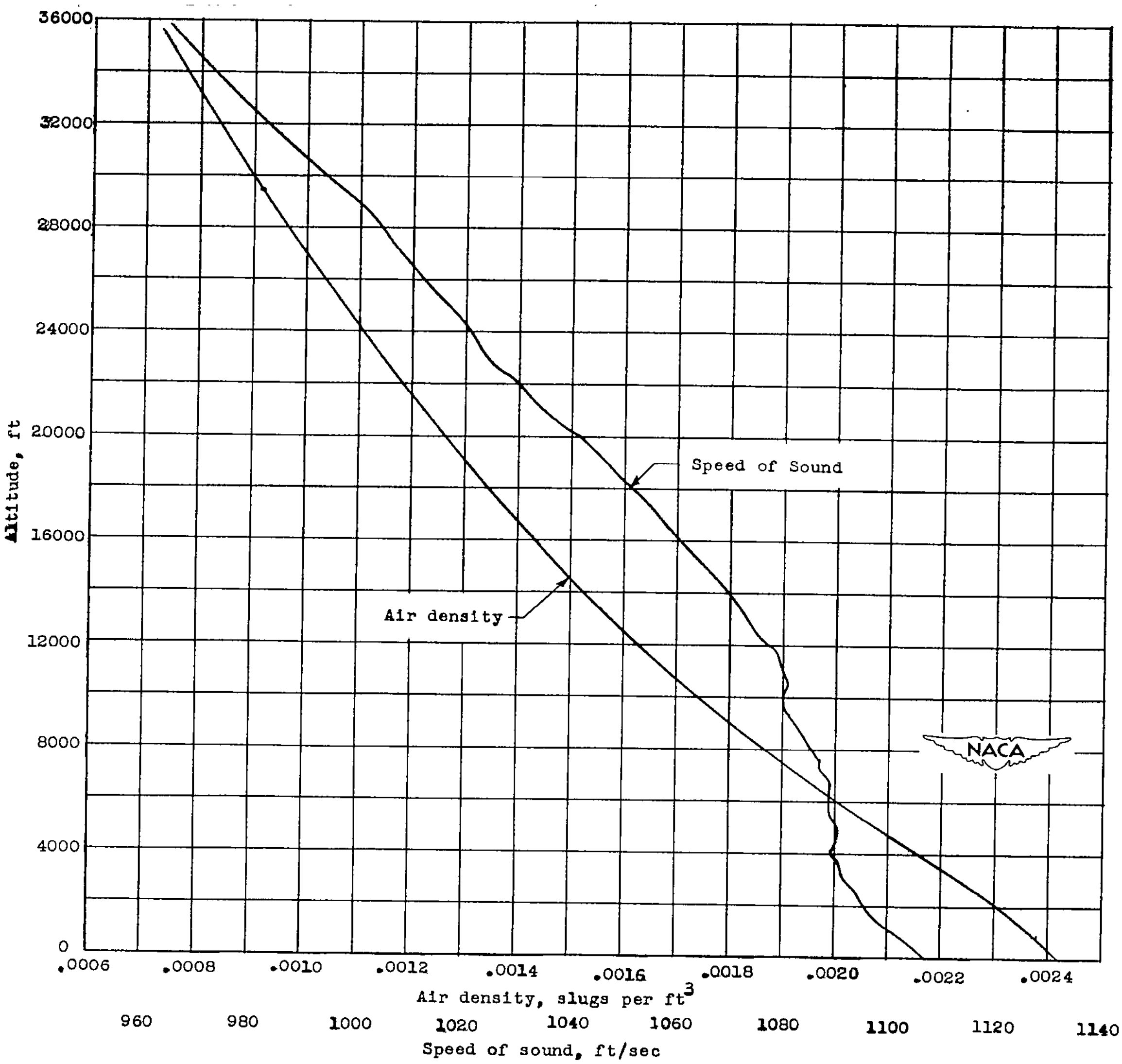

(b) Models 2, 3, 4, 5, and 6.

Figure 13.- Continued.

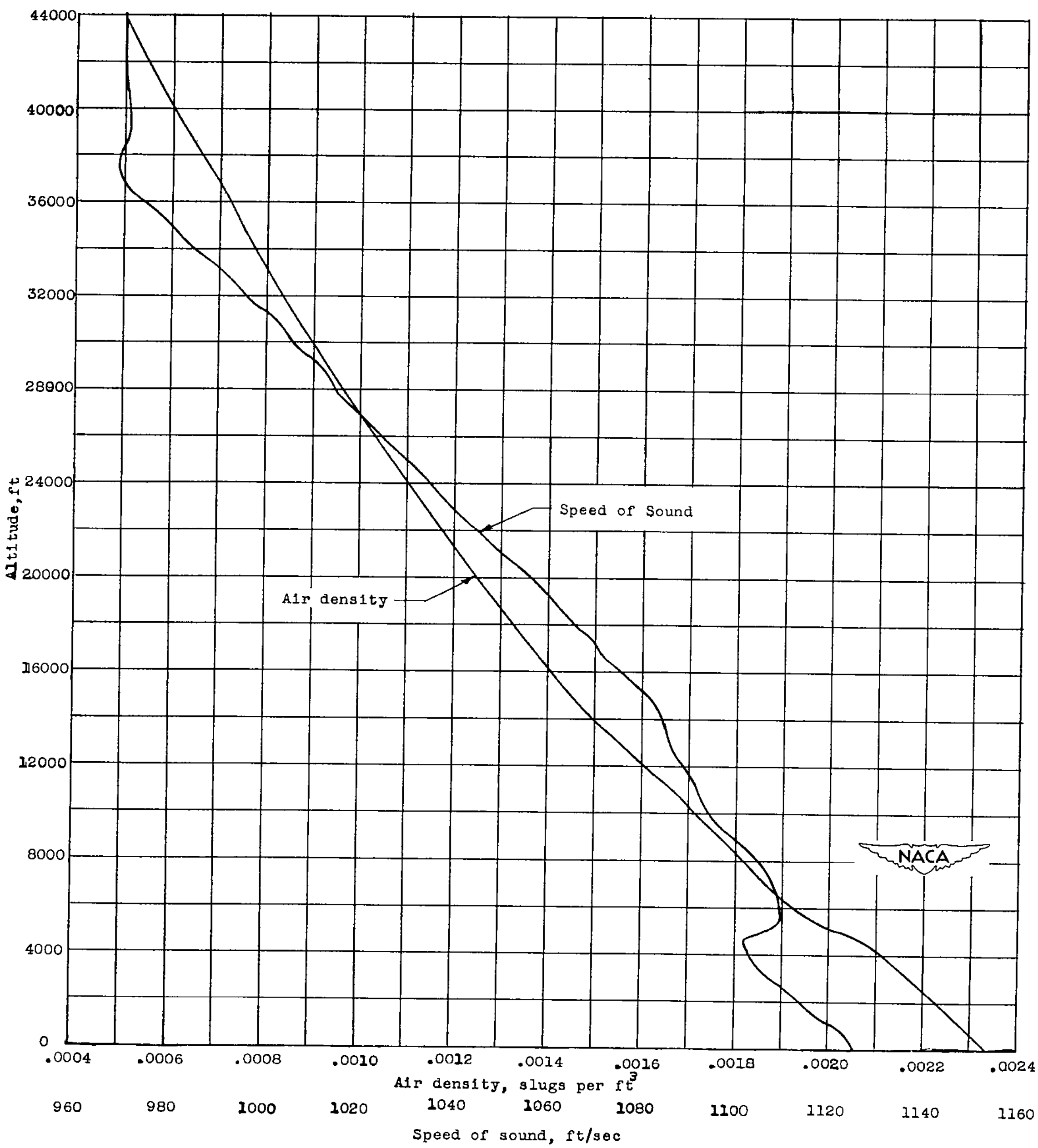

(c) Models 7, 8, and 9.

Figure 13.- Concluded.

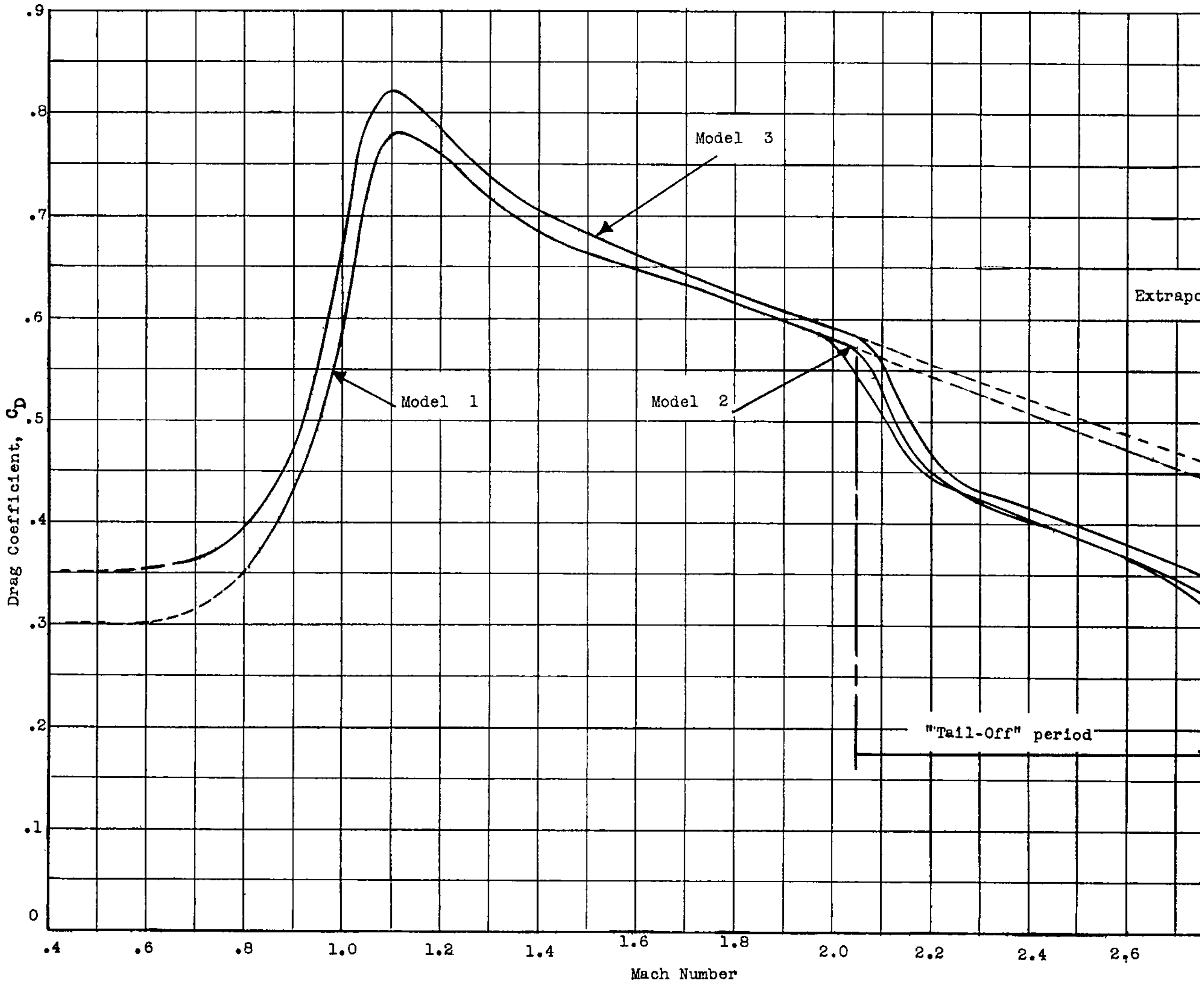

Figure 14.- Drag coefficient C_D for ambient models as a function of Mach number.

[redacted]

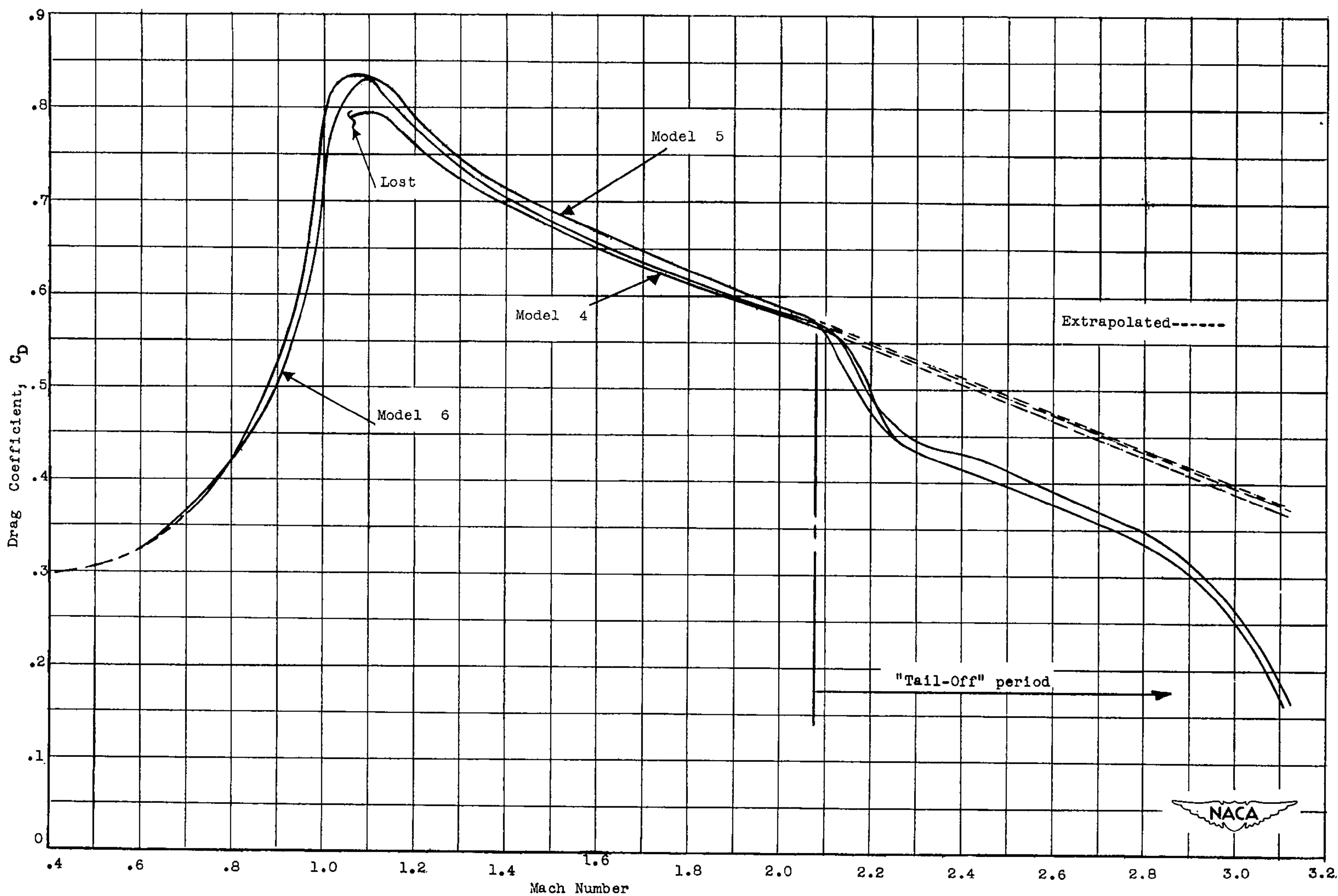

Figure 15.- Drag coefficient C_D for hot models as a function of Mach number.

[redacted]

[redacted]

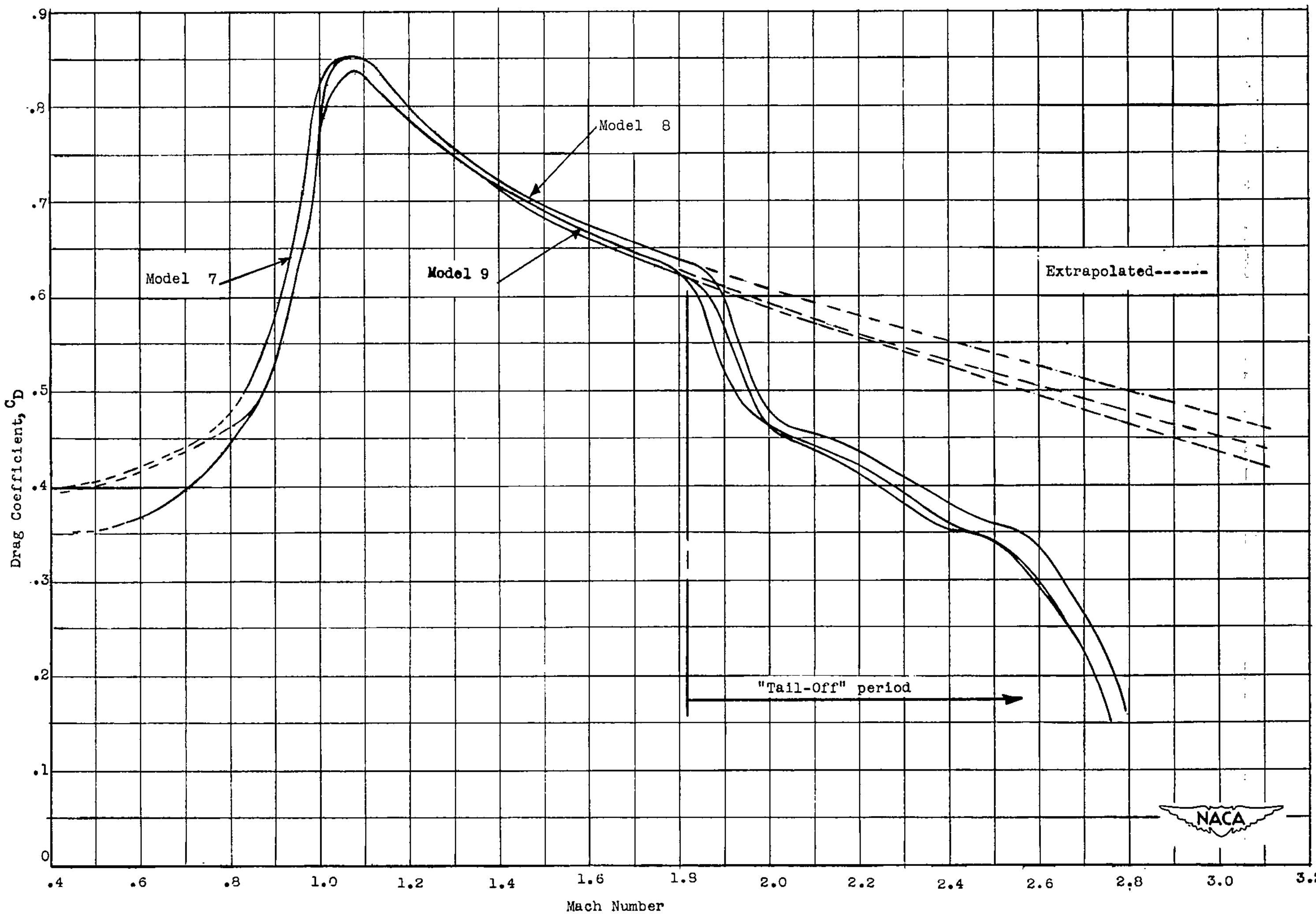

Figure 16.- Drag coefficient C_D for cold models as a function of Mach number.

[redacted]

[redacted]

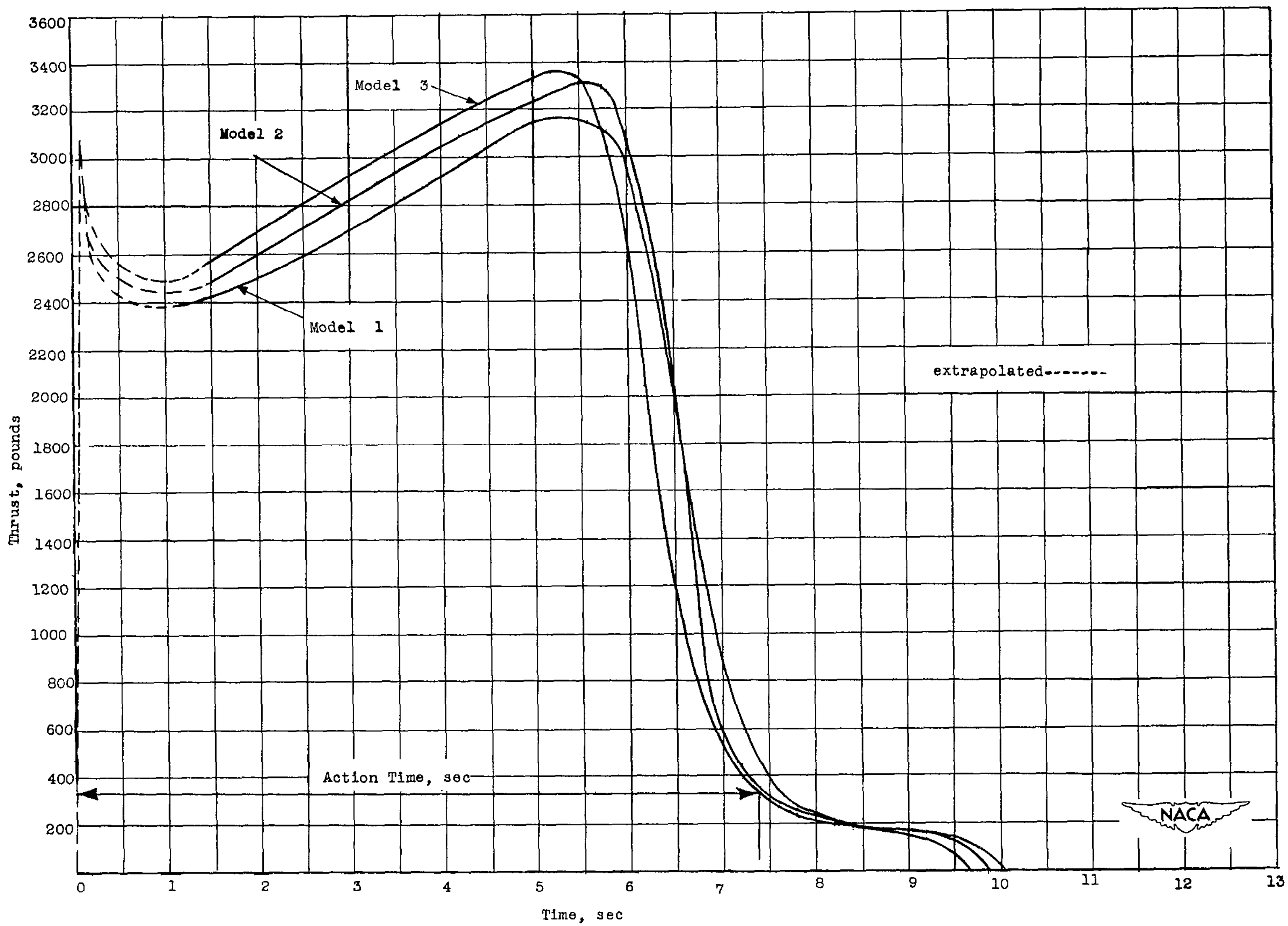

Figure 17.- Thrust for ambient models as a function of time.

[redacted]

[redacted]

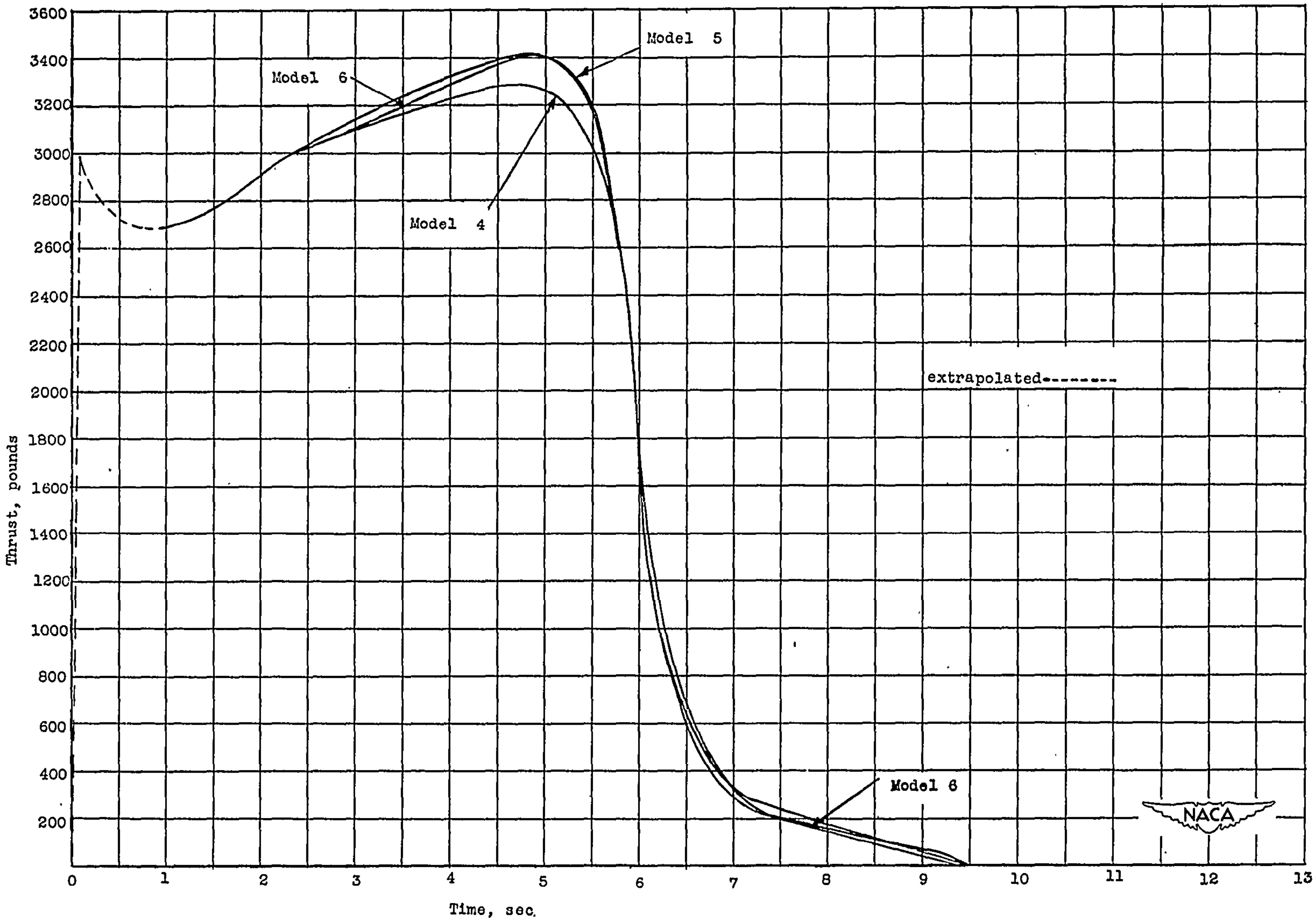

Figure 18.- Thrust for hot models as a function of time.

[redacted]

[redacted]

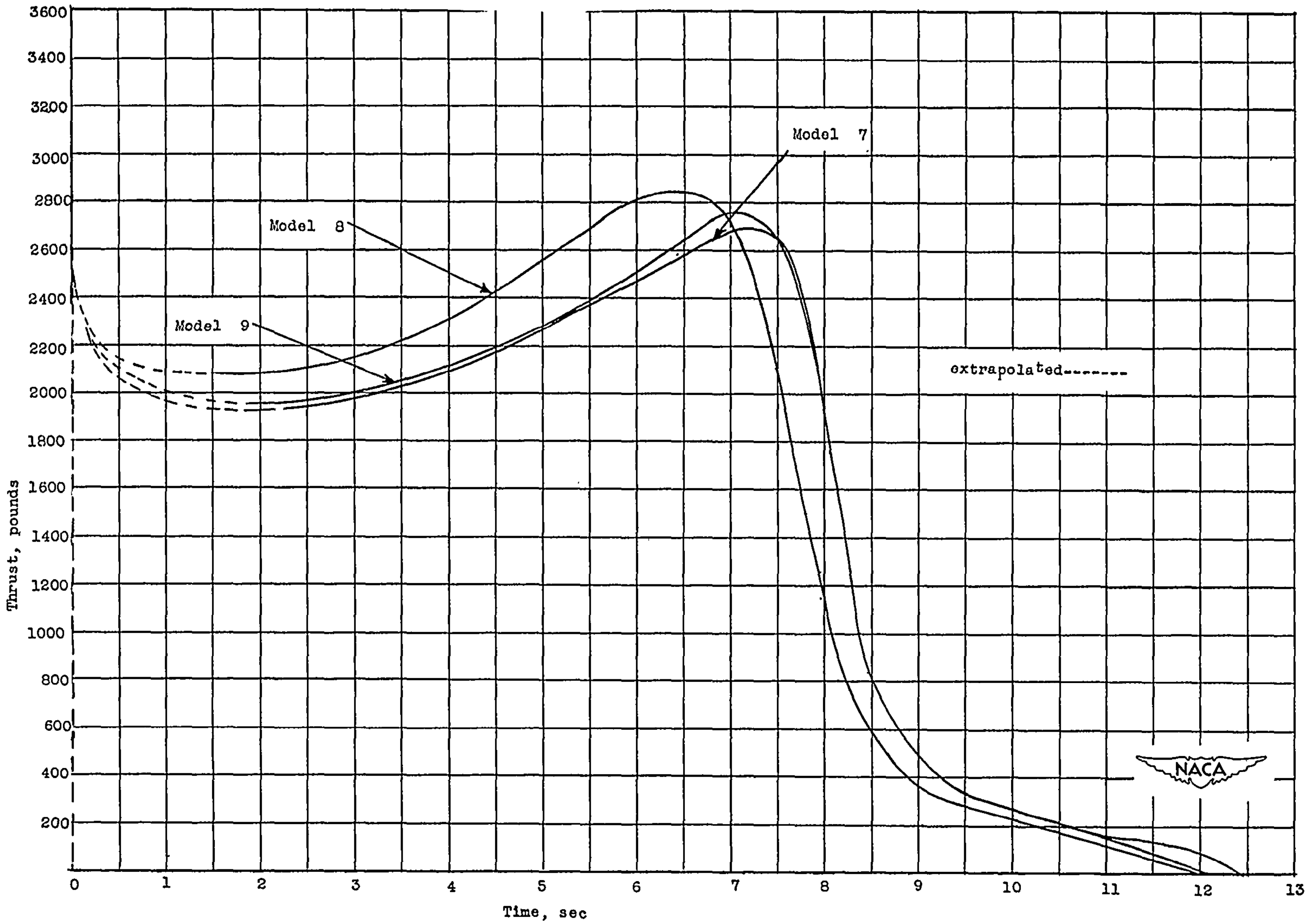

Figure 19.- Thrust for cold models as a function of time.

[redacted]

[redacted]

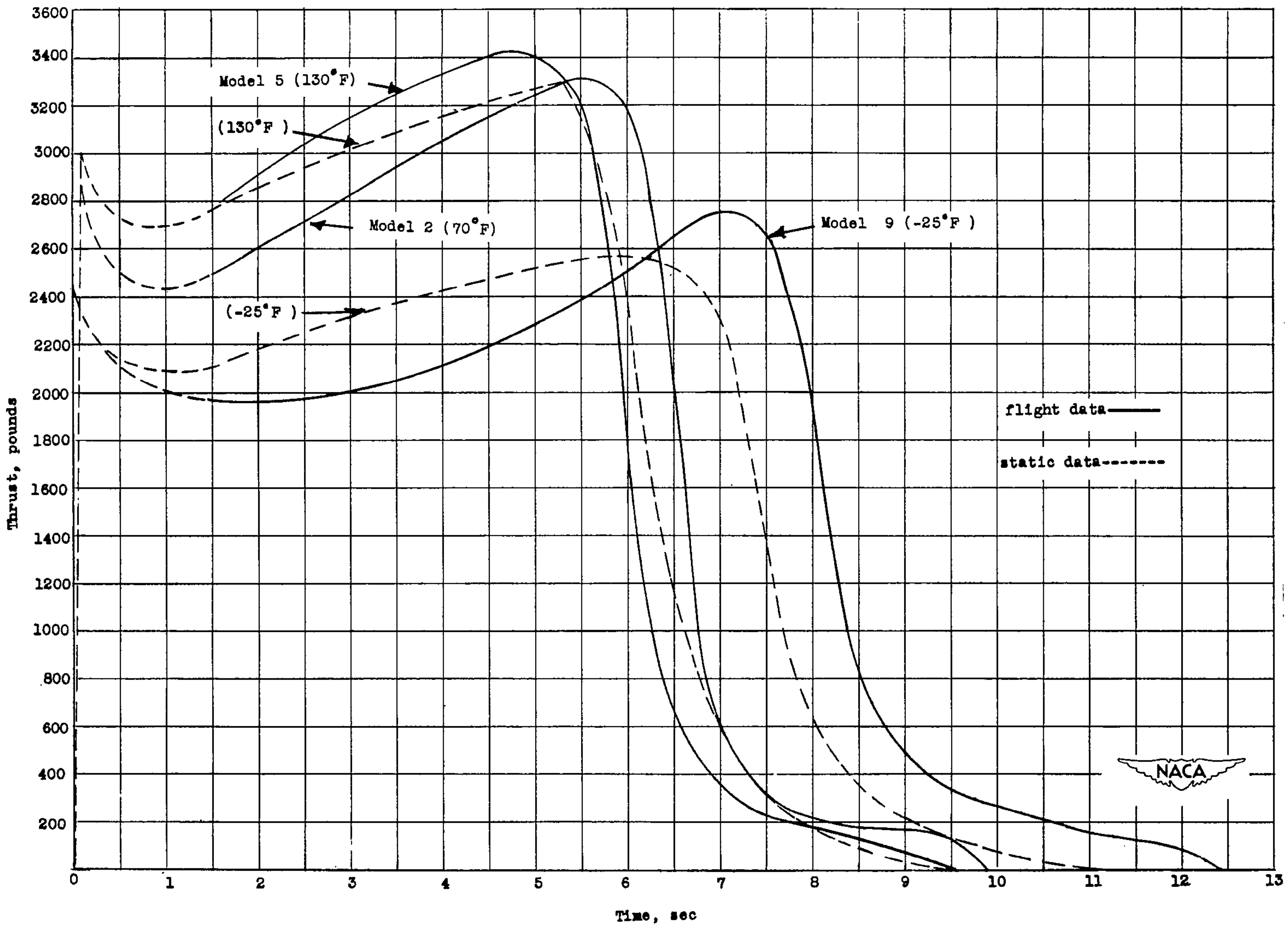

Figure 20.- Comparison of thrust curves obtained from flight and static tests.

[redacted]

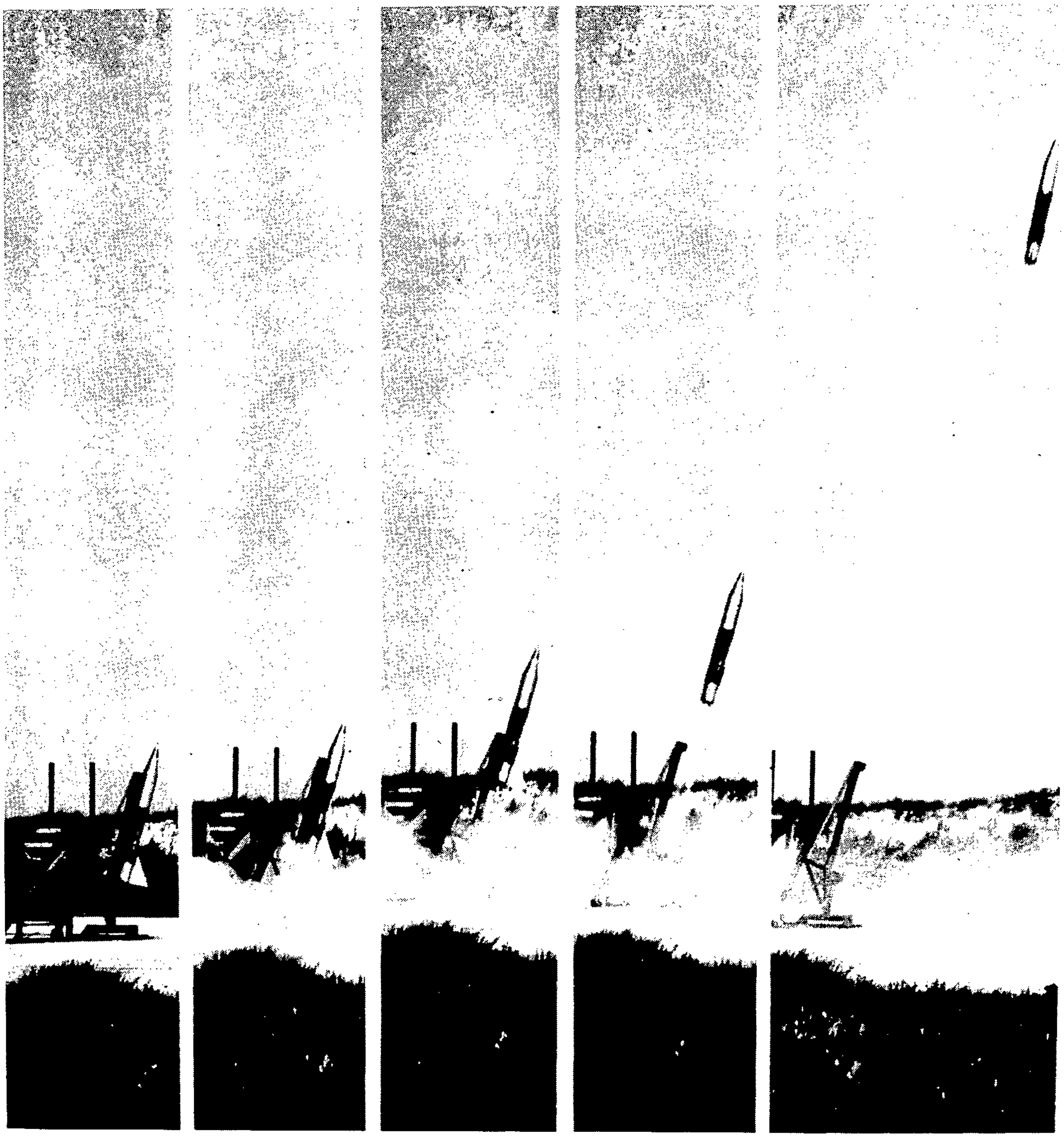

L-80269

Figure 21.- Sequence photographs of an ambient model at take-off.

SECURITY INFORMATION

[redacted]